

PCCP

Accepted Manuscript



This is an *Accepted Manuscript*, which has been through the Royal Society of Chemistry peer review process and has been accepted for publication.

Accepted Manuscripts are published online shortly after acceptance, before technical editing, formatting and proof reading. Using this free service, authors can make their results available to the community, in citable form, before we publish the edited article. We will replace this *Accepted Manuscript* with the edited and formatted *Advance Article* as soon as it is available.

You can find more information about *Accepted Manuscripts* in the [Information for Authors](#).

Please note that technical editing may introduce minor changes to the text and/or graphics, which may alter content. The journal's standard [Terms & Conditions](#) and the [Ethical guidelines](#) still apply. In no event shall the Royal Society of Chemistry be held responsible for any errors or omissions in this *Accepted Manuscript* or any consequences arising from the use of any information it contains.

Strain Tuning of the Charge Density Wave in Monolayer and Bilayer 1T-TaS₂

Li-Yong Gan^{a*}, Li-Hong Zhang^a, Qingyun Zhang^b, Chun-Sheng Guo^{a*}, Udo Schwingenschlögl^b, Yong Zhao^{a,c}

^aKey Laboratory of Advanced Technology of Materials (Ministry of Education), Superconductivity and New Energy R&D Center, Southwest Jiaotong University, Chengdu, Sichuan 610031, China

^bPSE Division, KAUST, Thuwal 23955-6900, Kingdom of Saudi Arabia

^cSchool of Materials Science and Engineering, University of New South Wales, Sydney, 2052 NSW, Australia

Corresponding Authors

*E-mails: wine_beer@163.com and csguo@swjtu.edu.cn.

Abstract

By first-principles calculations, we investigate the strain effects on the charge density wave states of monolayer and bilayer 1T-TaS₂. The modified stability of the charge density wave in the monolayer is understood in terms of the strain dependent electron localization, which determines the distortion amplitude. On the other hand, in the bilayer the effect of strain on the interlayer interaction is also crucial. The rich phase diagram under strain opens new venues for applications of 1T-TaS₂. We interpret the experimentally observed insulating state of bulk 1T-TaS₂ as inherited from the monolayer by effective interlayer decoupling.

1. Introduction

Layered transition metal dichalcogenides, such as $1T$ -TaS₂, $2H$ -TaSe₂, and $1T$ -TiSe₂, have received renewed interest in recent years due to a wealth of physics,¹⁻⁵ ranging from charge density waves (CDWs)^{6,7} to metal-insulator transitions⁸ and superconductivity.³ Particularly, $1T$ -TaS₂ has been extensively investigated because of its rich phase behavior as a function of the temperature.^{1, 3,4, 9-12} At 540 K an incommensurate CDW develops from the undistorted metallic structure, at 350 K an almost commensurate CDW is adopted, and further cooling to 180 K leads to a commensurate CDW, which exhibits a “Star-of-David” structure with an in-plane $\sqrt{13} \times \sqrt{13}$ periodic lattice distortion. The origin of the CDW, the pseudo-gapped Fermi surface, and the rich phase diagram are some of the topics that have motivated experimental and theoretical studies.^{3, 7, 9-13}

Recent progress in mechanical^{14,15} and chemical¹⁶ exfoliation enables the fabrication of planar $1T$ -TaS₂ samples as thin as a monolayer,¹⁷ initiating interest in the behavior of the CDW in two-dimensional systems.¹⁸⁻²⁰ It has been suggested that the CDW in the monolayer adopts the same periodic lattice distortion as known from the bulk. Specifically, inherent magnetism and semiconductivity coexist, distinguishing the monolayer fundamentally from the bulk as well as from other two-dimensional transition metal dichalcogenides.^{18,20} For the bilayer the CDW manifests a spin singlet insulator with the spins in the two layers forming a singlet state. On the other hand, for the bulk the origin of the insulating behavior^{1,2,4} remains an unsettled problem. While an insulating state was reproduced by dynamical mean-field theory,²¹ a recent theoretical study¹⁹ suggested a one-dimensional metallic state and indicated that the predictions of Ref. 22 are partly the consequence of an excessively large on-site

Coulomb parameter.

Control of the phase transitions and electronic properties of a material by means of external perturbations is critical for device applications. Strain engineering in this context is known to be an effective tool to tune the electronic properties in graphene²²⁻²⁵ and monolayer MoS₂,²⁶⁻²⁸ and other nanostructures.^{29,30} Additionally, strain is practically inevitable in nanostructures due to the lattice mismatch with the substrate.^{28, 31-33} For this reason, we investigate in the following how biaxial strain affects the CDW phases of monolayer and bilayer 1T-TaS₂. We demonstrate a series of phase transitions and analyze the corresponding material properties. In particular, our results allow us to explain the insulating behavior of bulk 1T-TaS₂.

2. Computational Details

First-principles calculations are performed using the Vienna Ab-initio Simulation Package with the spin-polarized generalized gradient approximation (Perdew-Burke-Ernzerhof). For both the monolayer and bilayer systems, $\sqrt{13} \times \sqrt{13}$ supercells are used to mimic strain effects on the “Star-of-David” clusters.¹⁸⁻²⁰ The kinetic energy cutoff is set to 500 eV and a Γ -centered $8 \times 8 \times 1$ k-mesh is used. The geometry is optimized until all residual forces have declined to less than 0.01 eV/Å. A damped van der Waals correction (D2)³⁴ is adopted to model nonbonding forces in the bilayer. In each case we apply a vacuum slab of at least 17 Å thickness to prevent unphysical interaction between periodic images. Test calculations with larger energy cutoffs and denser k-meshes have been performed and show that the presented results are fully converged. Additionally, an extra on-site Coulomb interaction with effective value $U - J = 2.27$ eV¹⁹ is considered to calculate the electronic structures.

3. Results and discussion

We first assess the properties of the CDW phases of unstrained monolayer and bilayer 1T-TaS₂. For the monolayer we introduce initial atomic displacements related to the soft phonon¹⁸ in the ideal system. After full relaxation the CDW is obtained. For the bilayer the CDW comes out spontaneously from the ideal geometry during the optimization. The results are summarized in Table I. For the monolayer and bilayer systems the CDW lowers the energy by 31 and 76 meV per formula unit, respectively. These values are much higher than those obtained without considering the van der Waals interaction,¹⁹ highlighting the significance of the interlayer interaction for the stability of the CDW in the bilayer case. The in-plane lattice constants are found to be the same. Moreover, the average distance between the two S layers in the monolayer and the average interlayer spacing in the bilayer amount to 3.075 and 2.971 Å, respectively. Figure 1 illustrates the optimized CDW structures. One can see the in-plane $\sqrt{13} \times \sqrt{13}$ periodic lattice distortions (“Star-of-David”), in which one Ta atom is located in the center of two rings with six Ta atoms each, consistent with previous studies.¹⁸⁻²⁰ Additionally, wave-like out-of-plane distortions are observed for the S layers in Figs. 1 (b) and (c). The displacements of the Ta atoms are substantial, up to 0.267 and 0.260 Å in the monolayer and bilayer systems, respectively. The monolayer shows a total magnetic moment of 1.0 μ_B , where most of the spin density is localized in the center of the “Star-of-David” cluster. The bilayer turns out to realize a spin singlet state (spin degeneracy).

Table 1. Energy difference per formula unit between the CDW and ideal phases (ΔE), in-plane lattice constant (a_0), maximum displacement of the Ta atoms (D_{Ta}), and total magnetic moment (M) for unstrained monolayer and bilayer 1T-TaS₂. Average distance between the two S layers in the monolayer ($\Delta_{\text{S-S}}$) and average interlayer spacing in the bilayer ($d_{\text{S-S}}$).

	ΔE (meV)	a_0 (Å)	$\Delta_{\text{S-S}}$ (Å)	$d_{\text{S-S}}$ (Å)	D_{Ta} (Å)	M (μ_B)
Monolayer	-31	12.151	3.075	-	0.267	1.0
Bilayer	-76	12.151	-	2.971	0.260	0

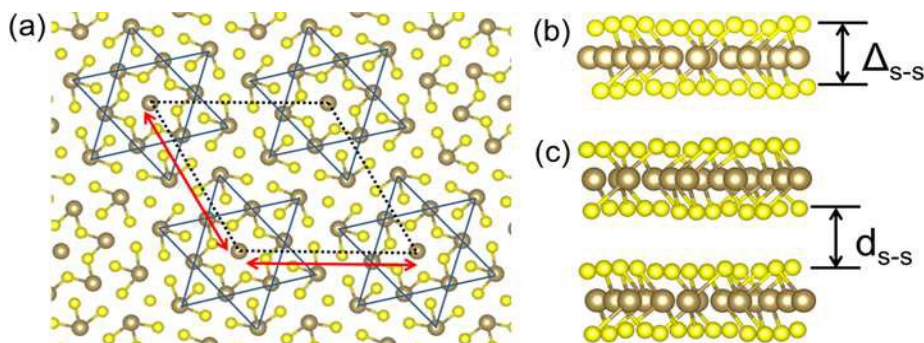


FIG. 1. (a) Top view of the CDW phase with $\sqrt{13} \times \sqrt{13}$ periodicity (dashed lines) in monolayer 1T-TaS₂. Red arrows indicate the direction of the biaxial strain. Side views of the CDW phase in (b) monolayer and (c) bilayer 1T-TaS₂. The Ta and S atoms are shown in brown and yellow, respectively.

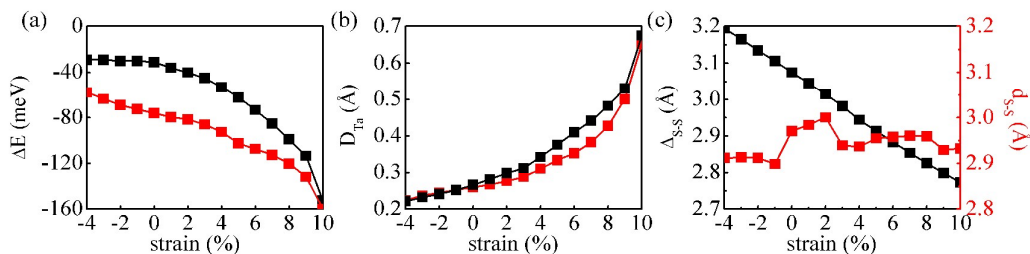


FIG. 2. Strain dependence: (a) Energy difference per formula unit, (b) maximum displacement of the Ta atoms in the monolayer/bilayer (black/red), and (c) average thickness of the monolayer (black) and average interlayer spacing in the bilayer (red).

In-plane biaxial compressive and tensile strains are applied to the monolayer and bilayer system. The energy difference between the CDW and ideal phases as a function of the strain is shown in Fig. 2 (a) to describe the effect on the stability of the CDW. Clearly, the CDW is energetically less favorable in the monolayer than in the bilayer under all considered strains. This relation is enhanced from -4% to 0% strain but reduced to almost zero at 10% strain, as in the monolayer the stability is slightly reduced by compression and remarkably enhanced by tension, while in the bilayer these effects are of comparable size. The finding that in the bilayer the CDW becomes less and less favorable, on the other hand, suggests a weakened interlayer interaction for increasing tension.

As the CDW leads to symmetry lowering,³⁵ we analyze in Fig. 2(b) the strain dependence of the distortion amplitude, given by the maximum displacement of the Ta atoms, D_{Ta} , to characterize the modified CDW stability from a structural perspective. Under tension the overlap between atomic orbitals is reduced, favoring the formation of a CDW.^{11, 35} As a result, for the monolayer the structural distortion is enhanced more and more, correlating with the trend of the stability. For the bilayer the displacements are very similar to those of the monolayer under compression, but much smaller under moderate tension, reflecting the role of the interlayer interaction in stabilizing the CDW. The average thickness of the monolayer varies linearly with the strain, whereas the behavior of the average interlayer spacing in the bilayer is complicated, with a minimum at -1% and a maximum at 2%, in an overall rather narrow range, see Fig. 2 (c).

Orbital polarization, which depends strongly on the strength of the electron correlations, leads to a symmetry lowering.³⁵ The strength of the correlations, on the other hand, is given

by the localization of the orbitals, which can be characterized by the bandwidth. Therefore, we present in Fig. 3 band structures under strain. For the monolayer compression hardly modifies the bandwidth of the valence states, except for -4% strain (explaining the slightly reduced stability of the CDW). For the bilayer, however, the bandwidth is clearly reduced, agreeing well with the observed stability variation. Upon tension the orbitals overlap less and the states localize so that the CDW is stabilized in both systems.

Our results show that the unstrained monolayer in the CDW structure is an insulator with a gap of 0.12 eV between two flat bands of opposite spin as a result of the periodic lattice distortion, while the bilayer is an insulator (0.16 eV) due to the formation of a singlet state.^{18,19} This can be regarded as a fully occupied bonding state and an empty antibonding state. As shown in Fig. 3, in the monolayer the two flat bands in the vicinity of the Fermi energy (E_F) remain nearly unchanged up to $\epsilon = 3\%$ and an insulating behavior is maintained with a virtually constant total magnetic moment of $1.0 \mu_B$. At 4% tension they develop dispersion and touch E_F , transforming the system into a spin gapless semiconductor³⁶ with a reduced total magnetic moment of $0.2 \mu_B$. From 5% to 10% strain the upper flat band shifts away from E_F and other valence bands shift up, giving rise to a magnetic semiconductor. The dispersion of both flat bands is reduced under increasing tension. For the bilayer, on the other hand, diamagnetism prevails. Compression enhances the dispersion of the valence band and the conduction band shifts to higher energy up to -1% strain and back thereafter up to 3% strain. Surprisingly, from 4% to 7% strain the system becomes magnetic and the band structure reveals clear similarity to that of the monolayer (except for the doubling of the bands seen in Fig. 3) with doubled magnetic moments. This behavior is ascribed to the fact that

larger strain weakens the interlayer interaction, as discussed in the following (compare Fig. 5), and thus the bonding-antibonding splitting, so that Hund's rule predicts two electrons with parallel spin. Both 4% and 8% tension transform the system into a magnetic metal. These novel features highlight the role of the interlayer interaction for the properties of the CDW, in agreement with a recent experimental report, in which a semiconductor-metal transition was obtained by modulating the orbital overlap in the bilayer.³⁷

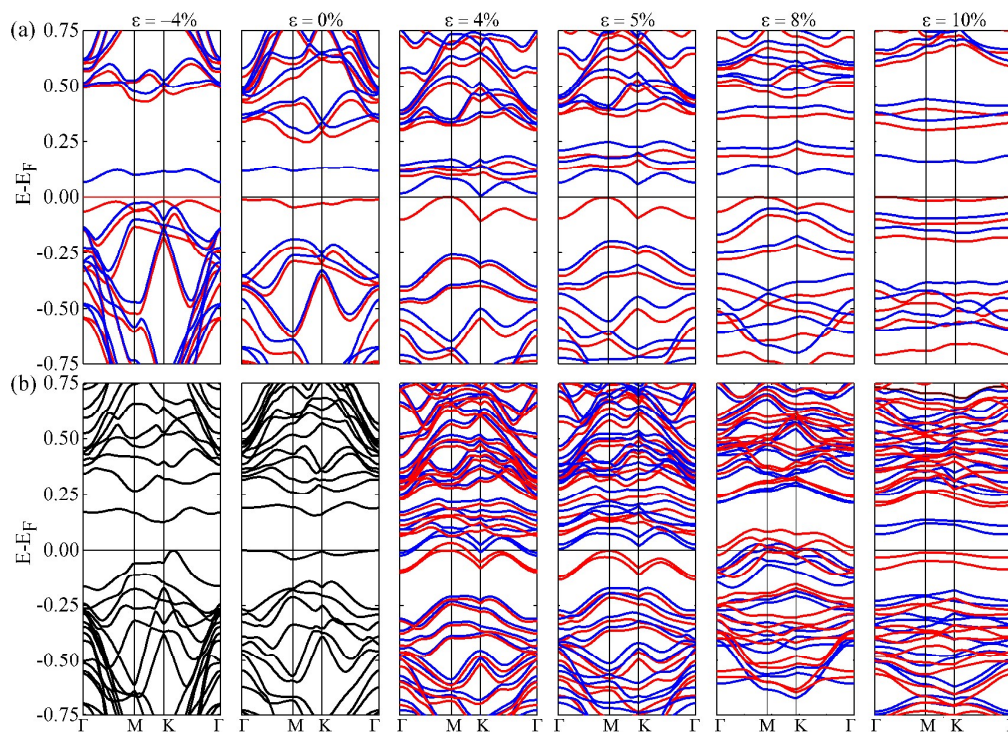


FIG. 3. Strain effect on the band structures of (a) monolayer and (b) bilayer $1T\text{-TaS}_2$ in the CDW structure. Red: spin-majority bands; Blue: spin-minority bands; Black: spin-degenerate bands.

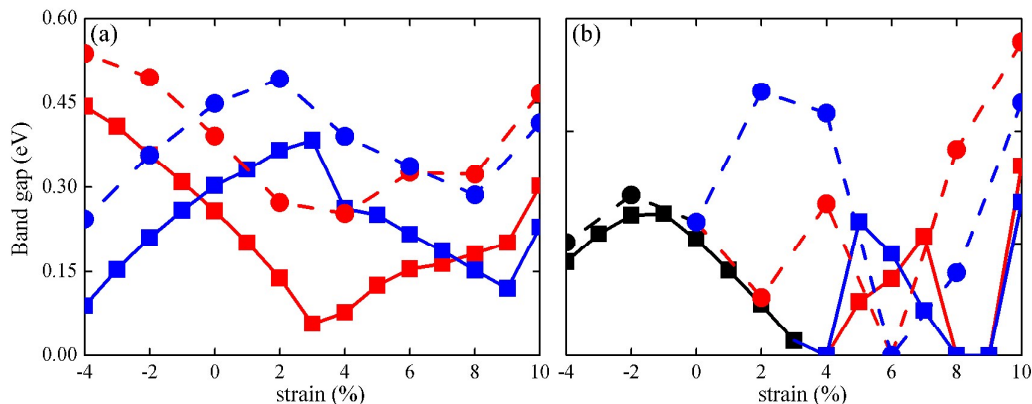


FIG. 4. Strain effect on the band gaps of (a) monolayer and (b) bilayer 1T-TaS₂ in the CDW structure. Red: spin-majority bands; Blue: spin-minority bands; Black: spin-degenerate bands. Dashed/solid lines: with/without on-site Coulomb interaction.

The band gap variation under strain is addressed in Fig. 4, separately for the two spin channels, in order to analyze the evolution of the magnetism. For the monolayer the band gap in the spin-majority channel decreases almost linearly from -4% to 3% strain and afterwards experiences two sharp steps up within a moderate and nearly linear upwards trend. In contrast, the band gap in the spin-minority channel increases to a maximum at 3% strain and then decreases up to 9% tension. Consequently, the magnetic semiconducting feature is maintained. For the bilayer the spin-degenerate band gap increases up to -1% strain due to the previously mentioned evolution of the conduction band and then shrinks up to 3% tension. At 4% strain a splitting is observed, resulting in a transition from an insulator to a magnetic metal. Increasing the tension from 5% to 7% leads to sizable band gaps in both spin channels, transforming the material into a magnetic semiconductor. Higher strain yields a magnetic metal, which reverts back into a magnetic semiconductor at 10% strain. When an on-site Coulomb interaction is included, see the dashed lines in Fig. 4, we find similar trends for the band gaps as a function

of the strain in the monolayer, except for the size of the band gaps. In the bilayer the trends are more complicated due to the interlayer interaction, but the magnetism is also recovered and phase transitions consistent with those found without an on-site Coulomb interaction are obtained. The appearance of magnetism suggests that proper tension is able to decouple the spins that form a singlet in the unstrained case.

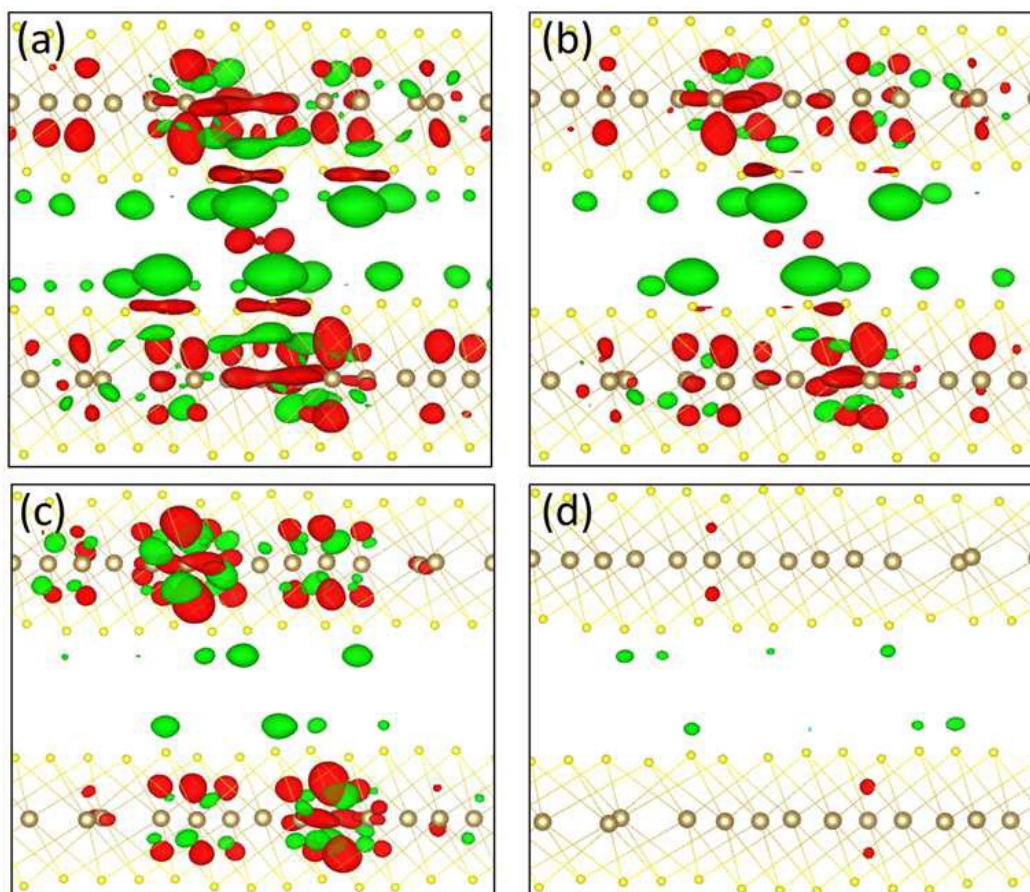


FIG. 5. Charge density differences for bilayer 1T-TaS₂ under (a) -3%, (b) 0%, (c) 3%, and (d) 6% strain. The isosurface value is 6.5×10^{-4} electrons/ \AA^3 . Red and green color, respectively, represents charge accumulation and depletion.

A recent theoretical study has demonstrated for the CDW phase of the monolayer a spin-1/2 Mott state and for the bilayer the formation of a spin singlet state, whereas the bulk constitutes a one-dimensional metal.¹⁹ However, the latter disagrees with the experimental observation of an insulating state,^{1,2, 4} which the authors explain by disorder effects. Our results suggest that proper strain can induce magnetism with a monolayer-like band structure in the bilayer. Unraveling this transition is useful for understanding the insulating state of the bulk. To this aim, we investigate the interlayer interaction by visualizing in Fig. 5 the charge redistribution upon bilayer formation from two isolated monolayers. In fact, the interaction is very weak, but still must account for the quenching of the magnetism in the bilayer. Given that the average interlayer distance is not sensitive to strain, a compression strengthens the interaction, so that the system remains in a spin singlet state and thus insulating. A tension of 3% remarkably weakens the interlayer interaction and localizes the in-plane states. At 4% tension these effects are strong enough to induce a phase transition into a magnetic state. Even larger strain further weakens the interlayer interaction, as shown for 6% strain, thus yielding a monolayer-like band structure for the bilayer. It has been reported that the stacking in the bilayer plays an important role for its electronic structure.³⁷ We thus consider another stacking choice for the CDW distortion in which the centers of the “Star-of-David” clusters in different layers line up. We find that 4% tension also leads to a transition from an insulator to a magnetic metal. Additionally, under tensile strain a similar stabilization of the CDW and a similar interlayer decoupling are obtained.

Based on our bilayer results, we conjecture that the insulating state of bulk 1T-TaS₂ may arise from interlayer decoupling caused by internal and/or external factors, such as strain. To

verify this hypothesis, we compare the band structures without strain and under 6% tension in Fig. 6. Without strain the out-of-plane states are remarkably coupled and the magnetism is suppressed, yielding one-dimensional metallicity (see the dispersion of the band crossing E_F along Γ -A).^{18,19} 6% tension raises the spin singlet state in energy and recovers magnetism, similar to the situation in the bilayer. At the same time the dispersion along Γ -A is strongly reduced and exhibits sizable band gaps in both spin channels, giving rise to a magnetic semiconductor, as for the monolayer. Though there are practical limitations in achieving large tensile strain, these findings demonstrate that such in-plane tension is able to decouple the interlayer interaction. As a result of internal and/or external factors (e.g., strain and stacking faults), the experimentally observed insulating state of bulk 1T-TaS₂ thus is a reminiscence of the monolayer properties.

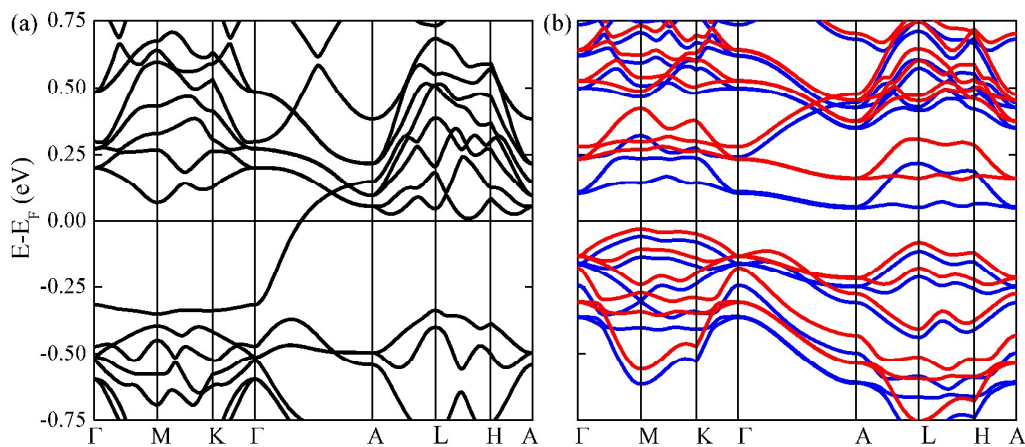


FIG. 6. Band structures of bulk 1T-TaS₂ (a) without strain and (b) under 6% tension. Red: spin-majority bands; Blue: spin-minority bands; Black: spin-degenerate bands.

4. Conclusions

In conclusion, first-principles calculations have been used to investigate the structural and electronic properties of the CDW structures of monolayer and bilayer 1T-TaS₂ under biaxial strain. In both systems the stability of the CDW is reduced and enhanced by compressive and tensile strain, respectively. The behavior of the monolayer can be explained purely by modifications of the electron localization under strain. On the other hand, in the bilayer the strain dependence of the interlayer interaction likewise plays a crucial role. It is a spin singlet insulator from -4% to 3% strain, but reveals magnetic semiconducting and magnetic metallic states between 4% and 10%. The recovered magnetism and the monolayer-like band structure are ascribed to weakening of the interlayer interaction under strain. Accordingly, an effective interlayer decoupling in bulk 1T-TaS₂ would allow us to understand the insulating state of this material as reminiscence of the monolayer properties.

ACKNOWLEDGMENTS

We acknowledge financial support of the National Natural Science Foundation of China (No.51302231) and the Fundamental Research Funds for the Central Universities (SWJTU2682013RC02, SWJTU11ZT31, 2682013CX004). Research reported in this publication was supported by the King Abdullah University of Science and Technology (KAUST).

References

1. L. Perfetti, A. Georges, S. Florens, S. Biermann, S. Mitrovic, H. Berger, Y. Tomm, H. Höchst, M. Gioni, *Phys. Rev. Lett.*, 2003, **90**, 166401.

2. L. Perfetti, P. A. Loukakos, M. Lisowski, U. Bovensiepen, H. Berger, S. Biermann, P. S. Cornaglia, A. Georges, M. Wolf, *Phys. Rev. Lett.*, 2006, **97**, 067402.
3. B. Sipos, A. F. Kusmartseva, A. Akrap, H. Berger, L. Forró, E. Tutiš, *Nat. Mater.*, 2008, **7**, 960-965.
4. L. Perfetti, P. A. Loukakos, M. Lisowski, U. Bovensiepen, M. Wolf, H. Berger, S. Biermann, A. Georges, *New J. Phys.*, 2008, **10**, 053019.
5. S. Hellmann, M. Beye, C. Sohrt, T. Rohwer, F. Sorgenfrei, H. Redlin, M. Kalläne, M. Marczyński-Bühlow, M. B. F. Hennies, A. Föhlisch, L. Kipp, W. Wurth, K. Rossnagel, *Phys. Rev. Lett.*, 2010, **105**, 187401.
6. J. A. Wilson, A. D. Yoffe, *Adv. Phys.*, 1969, **18**, 193.
7. J. A. Wilson, F. J. D. Salvo, S. Mahajan, *Adv. Phys.*, 1975, **24**, 117.
8. P. Fazekas, E. Tosatti, *Philos. Mag. Part B*, 1979, **39**, 229.
9. B. Dardel, M. Grioni, D. Malterre, P. Weibel, Y. Baer, F. Lévy, *Phys. Rev. B*, 1992, **45**, 1462(R).
10. R. E. Thomson, B. Burk, A. Zettl, J. Clarke, *Phys. Rev. B*, 1994, **49**, 16899.
11. A. Y. Liu, *Phys. Rev. B*, 2009, **79**, 220515(R).
12. Y. Yu, F. Yang, X. F. Lu, Y. J. Yan, Y.-H. Cho, L. Ma, X. Niu, S. Kim, Y.-W. Son, D. Feng, S. Li, S.-W. Cheong, X. H. Chen, Y. Zhang, *Nat. Nanotechnol.*, 2015, **10**, 270-276.
13. J. Zhang, R. Sknepnek, R. M. Fernandes, J. Schmalian, *Phys. Rev. B*, 2009, **79**, 220502(R).
14. K. S. Novoselov, D. Jiang, F. Schedin, D. J. Booth, V. V. Khotkevich, S. V. Morozov, A. K. Geim, *Proc. Natl. Acad. Sci. USA*, 2005, **102**, 10451.
15. B. Radisavljevic, A. Radenovic, J. Brivio, V. Giacometti, A. Kis, *Nat. Nanotechnol.*, 2011, **6**, 147-150.
16. J. N. Coleman, M. Lotya, A. O'Neill, S. D. Bergin, P. J. King, U. Khan, K. Young, A. Gaucher, S. De, R. J. Smith, I. V. Shvets, S. K. Arora, G. Stanton, H.-Y. Kim, K. Lee, G. T. Kim, G. S. Duesberg, T. Hallam, J. J. Boland, J. J. Wang, J. F. Donegan, J. C. Grunlan, G. Moriarty, A. Shmeliov, R. J. Nicholls, J. M. Perkins, E. M. Grievson, K. Theuwissen, D. W. McComb, P. D. Nellist, V. Nicolosi, *Science*, 2011, **331**, 568.
17. H. Li, G. Lu, Y. Wang, Z. Yin, C. Cong, Q. He, L. Wang, F. Ding, T. Yu, H. Zhang, *Small*, 2013, **9**, 1974-1981.
18. Q. Zhang, L.-Y. Gan, Y. Cheng, U. Schwingenschlögl, *Phys. Rev. B*, 2014, **90**, 081103(R).
19. P. Darancet, A. J. Millis, C. A. Marianetti, *Phys. Rev. B*, 2014, **90**, 045134.
20. X.-L. Yu, D.-Y. Liu, T. Jia, H.-Q. Lin, L.-J. Zou, *arXiv:1407.1407*.
21. J. K. Freericks, H. R. Krishnamurthy, Y. Ge, A. Y. Liu, T. Pruschke, *Phys. Status Solidi B*, 2009, **246**, 948-954.
22. M. Mohr, K. Papagelis, J. Maultzsch, C. Thomsen, *Phys. Rev. B*, 2009, **80**, 205410.
23. G. Cocco, E. Cadelano, L. Colombo, *Phys. Rev. B*, 2010, **81**, 241412(R).
24. Y. C. Cheng, Z. Y. Zhu, G. S. Huang, U. Schwingenschlögl, *Phys. Rev. B*, 2011, **83**, 115449.
25. A. L. Kitt, V. M. Pereira, A. K. Swan, B. B. Goldberg, *Phys. Rev. B*, 2012, **85**, 115432.
26. J. Feng, X. Qian, C.-W. Huang, J. Li, *Nat. Photon.*, 2012, **6**, 866-872.
27. P. Johari, V. B. Shenoy, *ACS Nano*, 2012, **6**, 5449-5456.
28. K. He, C. Poole, K. F. Mak, J. Shan, *Nano Lett.*, 2013, **13**, 2931-2936.
29. C.-S. Guo, M. A. Van Hove, *J. Phys. Chem. C*, 2011, **115**, 4516-4522.

30. L. Zhang, X. Xin, C.-S. Guo, L.-Y. Gan, Y. Zhao, *Solid State Commun.*, 2015, **207**, 26-29.
31. Z. H. Ni, T. Yu, Y. H. Lu, Y. Y. Wang, Y. P. Feng, Z. X. Shen, *ACS Nano*, 2008, **2**, 2301-2305.
32. D. Svetin, I. Vaskivskyi, P. Sutar, J. Gospodaric, T. Mertelj, D. Mihailovic, *arXiv:1406.1427*.
33. F. Guinea, M. I. Katsnelson, A. K. Geim, *Nat. Phys.*, 2010, **6**, 30-33.
34. S. Grimme, *J. Comput. Chem.*, 2006, **27**, 1787-1799.
35. Z. Zhu, Y. Cheng, U. Schwingenschlögl, *Phys. Rev. B*, 2012, **85**, 245133.
36. X. L. Wang, *Phys. Rev. Lett.*, 2008, **100**, 156404.
37. T. Ritschel, J. Trinckauf, K. Koepernik, B. Buchner, M. V. Zimmermann, H. Berger, Y. I. Joe, P. Abbamonte, J. Geck, *Nat. Phys.*, 2015, **11**, 328-331.

Graphical Abstract



Analysis of monolayer and bilayer $1T\text{-TaS}_2$ suggests that the insulating state of the bulk is a consequence of interlayer decoupling.